Author Manuscript

Author Manuscript

Author Manuscript

Author Manuscript

HHS Public Access

Author manuscript

Technology (Singap World Sci). Author manuscript; available in PMC 2018 May 07.

Published in final edited form as:

Technology (Singap World Sci). 2017 December ; 5(4): 201–213. doi:10.1142/S233954781750011X.

Cell-sized lipid vesicles for cell-cell synaptic therapies

D. Vallejo[1], **S.H. Lee**[1], **D. Lee**[3], **C. Zhang**[3], **C. Rapier**[1], **S.D. Chessler**[3], and **A.P. Lee**[1,2]

[1]Department of Biomedical Engineering, University of California at Irvine, 3120 Natural Science II, Irvine, California 92697, USA

[2]Department of Mechanical and Aerospace Engineering, University of California at Irvine, 3120 Natural Science II, Irvine, California 92697, USA

[3]School of Medicine, University of California at Irvine, 1001 Health Sciences Rd, Irvine, CA, 92617, USA

Abstract

Cell-sized lipid vesicles (CLVs) have shown great promise for therapeutic and artificial cell applications, but their fragility and short shelf life has hindered widespread adoption and commercial viability. We present a method to circumvent the storage limitations of CLVs such as giant unilamellar vesicles (GUVs) and single-compartment multisomes (SCMs) by storing them in a double emulsion precursor form. The double emulsions can be stored for at least 8 months and readily converted into either GUVs or SCMs at any time. In this study, we investigate the interfacial parameters responsible for this morphological change, and we also demonstrate the therapeutic potential of CLVs by utilizing them to present a transmembrane protein, neuroligin-2, to pancreatic β-cells, forming cell-cell synapses that stimulate insulin secretion and cellular growth.

Keywords

Artificial Cells; Droplet Microfluidics; Giant Unilamellar Vesicles; Dewetting; Double Emulsions

INNOVATION

Cell-sized lipid vesicles (CLVs) can mimic the intercellular and intracellular functions of biological cells for cell-based therapies, biosensors, and bioreactors. One powerful intercellular function is the formation of cell-cell synapses to activate cells for therapeutic purposes. However, the fragility and short shelf life of CLVs render them difficult to ship and commercialize, limiting their use to very controlled laboratory settings. For GUVs and SCMs to realize their vast potential, it is paramount that they can be produced in bulk and stored for an extended time without structural degradation. Here we present a method to circumvent these limitations by storing double emulsion templates that can be converted to

Correspondence should be addressed to A.P.L. (aplee@uci.edu).

CONFLICTS OF INTEREST

There are no conflicts to declare.

Author Manuscript Author Manuscript Author Manuscript Author Manuscript

CLVs on demand by exposure to salt solutions that promote dewetting to produce lipid bilayer membranes.

INTRODUCTION

Functionalizing the surface of cell-sized particles with molecular structures that can initiate surface-surface contacts with living cells is of high interest for developing applications in medicine and synthetic biology. Intercellular communication is a fundamental feature of life, and the ability to exploit it can be used to effectively elicit a specific cellular response. Although several different mechanisms of cellular communication exist, the most commonly exploited are secretory (endocrine and paracrine) and juxtacrine signaling. Juxtacrine signaling involves the direct surface interaction between neighboring cells, and is of particular interest for medicine and therapeutics, as it plays a critical role in the body's immune response and in the development of various organs. Typical artificial cells imbued for biomimetic juxtacrine applications are normally solid structures that include microbeads (latex[1,2] and magnetic beads[3]) and hydrogel beads[4]. Though these solid structures can lend themselves well to certain biomimetic interactions, they fall short of imitating the fluidity and clustering of surface components seen in natural cell surface interactions, which can be critical to certain signaling pathways. The arrangement of ligand-receptor pairs into ordered spatial patterns during cell-cell contact is a recurring theme in many juxtacrine-signaling pathways, and in some cases, is absolutely necessary[5–7]. For example, the importance of fluid micro-domains in cell-to-cell communication is widely recognized in the immune synapse formed when antigen-presenting cells interact with T-cells, and is a prominent design criterion in the creation of artificial antigen presenting cells (aAPCs) for immunotherapy[8]. The neurexin-neuroligin signaling pathway is another network recently discovered to rely on ligand-receptor clustering and membrane fluidity, and plays a critical role in neuronal synapse formation[9].

Lipid vesicles are ideal candidates to replicate the fluidity of natural cell membranes, as they are constituted of identical materials. Vesicles are spherical capsules that have an internal aqueous compartment enclosed by semi-permeable, unilamellar or multi-lamellar lipid bilayers and their size can range from tens of nanometers to hundreds of microns in diameter. Due to their similarity to biological cells, they have also been used as models for various studies on the dynamic behavior of cellular membranes[10–14], and are popular candidates for which to build artificial cells[15–18]. Vesicles also lend themselves well to secretory signaling and drug delivery, as they can carry hydrophilic compounds in their aqueous core, and hydrophobic compounds can be incorporated within the hydrophobic region of the lipid bilayer. The polar head groups of the lipid surface can also be functionalized with various linker molecules to attach biological active compounds, proteins, antibodies, and nanomaterials. Though phospholipid vesicles are a popular platform to create artificial cells, a major drawback to cell-sized vesicles (giant unilamellar vesicles, or GUVs) is that they tend to be fragile and have a limited shelf life, currently limiting their use to research studies and short-term experiments. To realize the full capabilities of what an artificial cell can offer in a therapeutic and commercial sense, they should be able to be easily designed to survive in a wide variety of environments and conditions.

Author Manuscript Author Manuscript Author Manuscript Author Manuscript

Here, we report a method to circumvent the fragility and storage limitations of GUVs and demonstrate that they can be functionalized to elicit therapeutically relevant biological responses from mammalian cells. Specifically, we demonstrate continuous production of monodisperse double emulsions with tunable diameters (9–30 μm) and high generation rates (200–3,000 Hz) that can be stored for at least 8 months. On demand, they can be converted into lipid vesicles through proper interfacial tension manipulation via the use of electrolytes and surfactants. Here, we examine the critical interfacial forces that lead to dewetting of the double emulsion oil layer into an oil cap, and the subsequent removal of the oil cap. To validate its biological function, we successfully demonstrate increased stimulation of insulin secretion and cellular growth in pancreatic β cells by incubation with vesicles surface functionalized with neuroligin-2 (NL-2), a β cell transmembrane protein. This technology opens up a new paradigm for engineering artificial cells for biological studies and cell-based therapies.

METHODS

Materials

The internal aqueous solution consisted of a 1:1 mixture of deionized water and pluronic F68 (1%, 5%, or 10% solution, Sigma Aldrich) and 250 mM sucrose or 1× PBS (Fisher Scientific). The lipid-oil solution consisted of 10 mg ml^{-1} of DOPC (1,2-dioleoyl-sn-glycero-3-phosphocholine, Avanti Polar Lipids) and 5 mg ml^{-1} cholesterol (Avocado Research Chemicals, Ltd) dissolved in oleic acid (Fisher Scientific), unless otherwise noted. The external aqueous solution consisted of 2 parts (v/v) pluronic F68 (10% solution, Sigma Aldrich), 1 (v/v) part glycerol (EMD Biosciences), and 125 mM NaCl (Fisher Scientific). The double emulsions were stored in a 250 mM sucrose solution with 1% F68 pluronic. All experiments on CLV formation were performed using double emulsions that were stored for at least 1 month. *In vitro* experiments used double emulsions that were stored for at least one week before functional molecule conjugation and conversion into CLVs.

Photolithography and device fabrication

All devices were fabricated in poly(dimethyl) siloxane (PDMS) using standard soft lithography techniques[19]. Briefly, channel geometries were designed in AutoCAD (Autodesk) and Adobe Illustrator (Adobe) and printed at 20,000 dpi onto a transparency mask by CAD/Art Services (Bandon, OR). In a class 1000 cleanroom, a 3-inch silicon wafer was spin-coated with a 20 μm thick layer of SU-8 (2050, MicroChem) photoresist, and patterned with the photomask through exposure to UV light. After post-exposure baking, the silicon wafer was submerged in SU-8 developer to remove the unexposed photoresist. The remaining SU-8 formed the positive channel features on the silicon wafer. Wafers were then hard-baked at 150 °C for 5 minutes to harden and improve adhesion of the SU-8 to the wafer.

The wafers were spin-coated with 1% (v/v) Teflon® AF (DuPont™) in Fluorinert™ FC-43 (3M™) to reduce adhesion of PDMS to the wafer. PDMS (Sylgard 184, Dow Corning) was mixed at a ratio of 10:1 (w/w) pre-polymer base to curing agent, degassed for 30 minutes, and then poured onto the patterned silicon wafer. The polymer mixture was cured at 65 °C

Author Manuscript Author Manuscript Author Manuscript Author Manuscript

overnight. After curing, devices were cut out and inlet/outlet tubing holes were punctured into the device using disposable biopsy punches (Integra™ Miltex®). The PDMS devices were then cleaned and treated with pure air plasma (Harrick Scientific, NY) for 45 seconds at 300 mTorr to allow for irreversible bonding to a glass slide (Corning).

Hydrophilic surface treatment

Due to the inherent hydrophobic nature of PDMS, a selective hydrophilic surface treatment was applied immediately after bonding to the external phase channel to render the channel permanently hydrophilic.[20,21] The treatment promotes proper double emulsion production by ensuring that the external aqueous solution wets the walls of the microchannel at the droplet generation junction. Briefly, a vacuum was applied to the outlet of the device, and 1 μL of a 0.4 wt. % PVA (polyvinyl alcohol, average MW 30,000–70,000, 87%–90% hydrolyzed, Sigma Aldrich) solution was passed through the external phase channels. Once the liquid cleared from the channels (within 30 s), 5 μL of a 0.1% PVA solution was passed through the external phase channels to remove any PVA crystals that may have formed at the generation junction during the first application. The vacuum was left on for 2 minutes afterwards to ensure complete removal of the PVA solution from the channels. The device was then cured overnight at 120 °C.

Microfluidic experimental setup

Powdered lipid and cholesterol were dissolved in oleic acid to achieved desired concentration, with the aid of a 10-minute sonication bath at 40 °C. All solutions were sealed in 1.5 mL plastic microtubes (Phenix Research Products) and controlled via a pump system similar to that utilized by Martz *et al*.[22] Briefly, two lengths of Tygon tubing (Cole-Parmer) were inserted into holes drilled into the cap of the microtubes and glued into place to create an airtight seal. One length of tubing remained in the pressure headspace above the reagent and was connected at the other end to a SMC ITV0011-2UMS digital regulator (Automation Distribution) that was controlled via a custom LabView VI. Another length of tubing was submerged in the reagent solution with the other end connected to the appropriate inlet of the microfluidic device. By manually applying a positive pressure head to the reagent vial via the SMC digital regulator, fluid was driven through the channels of the microfluidic device. A length of Tygon tubing was also inserted in the outlet and placed in a microtube for collection of the double emulsions. Interfacial tensions between fluid phases were measured via the pendant drop technique using the Attension Theta Lite Tensiometer (Biolin Scientific) and accompanied software.

Device characterization and CLV formation

The external phase was driven via a digitally controlled syringe pump (Pico Plus, Harvard Apparatus). The sum of the flow-rates for the oil and internal aqueous phases was estimated from the droplet diameter and generation frequency. All measurements for characterization were accomplished on a device with a channel height of 20 μm and an orifice width of 15 μm. The population of the double emulsions was counted using a hemocytometer. Double emulsions in storage solution were mixed with 10 parts dewetting solution to initiate double emulsion oil phase dewetting and CLV formation. The dewetting solution was either a 125 mM solution of sodium acetate (EMD Chemicals Inc.) or 1× PBS (Gibco®).

Author Manuscript Author Manuscript Author Manuscript Author Manuscript

Analysis and imaging

Images and movies were captured using an inverted Nikon microscope and a high-speed camera (V310 Phantom, Vision Research). Excitation of the encapsulated fluorescent probe fluorescein was achieved with illumination from a mercury lamp through using a 475 nm FITC filter. Imaging of the probe was performed with an inverted fluorescent microscope (Nikon) at 40× magnification and captured with a high-resolution camera (Canon EOS 5D Mark III). ImageJ (NIH) was used for analyzing video and image data and making measurements.

Recombinant NL-2

INS-1 832/13 β cells were cultured in RPMI 1640 medium with 10% FBS, 2 mM L-glutamine, 1 mM sodium pyruvate, 50 μM β-mercaptoethanol, and penicillin-streptomycin. HEK293 cells stably transfected to express recombinant soluble NL-2, with an N-terminal FLAG epitope tag and C-terminal IgG Fc domain, and were cultured in DMEM with 10% FBS, 2 mM L-glutamine, and G418 sulfate as previously described[23].

Recombinant soluble NL-2 was purified from the medium of the stably transfected HEK293 cells using ANTI-FLAG® M2 affinity gel (Sigma-Aldrich) as described previously[23]. To create the functionalized SCMs, double emulsions were first prepared using 5% molar 1,2-distearoyl-sn-glycero-3-phosphoethanolamine-N-[amino(polyethyleneglycol)-2000] (ammonium salt) (Avanti Polar Lipids) in a 3:1 molar ratio of DOPC to DPPC (10 mg/mL total lipid for DOPC/DPPC mixture) in oleic acid with 5 mg/mL cholesterol. An aqueous solution of EDC (100 mg/mL, 200 mL) and NHS (100 mg/mL, 200 mL) was added to the NL-2 protein (0.172 mg/mL, 500 mL) solution for a 30-minute incubation. Double emulsions were then added to the solution (100:1 molar ratio of protein to vesicles) for 4 hours of conjugation. Afterwards, the double emulsions conjugated with NL-2 were washed three times in storage solution (PBS with 1% pluronic F68) to remove unconjugated protein. The double emulsions were converted into SCMs, after which they were added to the culture medium to perform cellular studies.

Assessment of glucose-stimulated insulin secretion and cell growth by vesicle-treated INS-1 832/13 β-cells

Naked vesicles (control) or NL-2 vesicles were added to the culture medium of INS-1 832/13 cells grown to 40%–50% confluence on 24-well plates. After 24-hour incubation with vesicles, 832/13 cells were starved for 1 hour with 2.75 mM glucose in Krebs-Ringer bicarbonate buffer (KRB). Stimulated insulin secretion was then assessed as previously described[24]. Briefly, insulin secretion was stimulated for 1 hour with 16.7 mM glucose and 100 μM IBMX in KRB. Secreted and cellular insulin levels were then determined by a radioimmunoprecipitation (RIPA) assay (EMD Millipore). For assessment of vesicular effects on cell growth, INS-1 832/13 cells were grown to 25%–35% confluence before 24-hour vesicle incubation. Total cellular protein levels were assessed with DC Protein Assay (Bio-Rad).

Author Manuscript Author Manuscript Author Manuscript Author Manuscript

Insulin secretion dose-response curves were analyzed with MAT-LAB (MathWorks) by one-way ANOVA. Pairwise comparisons were determined with a Bonferroni correction. Protein levels were analyzed by an independent *t*-test.

RESULTS

Double emulsion production and storage

The device (Fig. 1a) is designed to produce W/O/W double emulsions at a single flow-focusing junction[25]. The external phase channel is rendered hydrophilic with a PVA surface treatment as described previously[21], while the oil and internal phase channels remain hydrophobic. The hydrophobic channel wall ensures that the oil phases sheaths the internal aqueous phase before reaching the droplet generation region. The hydrophilic external phase channel wall then allows sheathing of the oil phase by the external aqueous solution before droplet breakoff.

Production results are summarized in Fig. 1b–e. In our experiments, the flow of the oil phase was maintained such that each water droplet was encased in a very thin (~1–3 μm thick) oil shell. Figure 1b plots double emulsion diameter (D, μm), normalized to orifice width (D_0), as a function of the external phase flow-rate (Q_{Ext}) normalized to the sum of the oil and internal phase flow-rates (Q_{Disp}), simplifying the analysis to that of single emulsion production. The data is fitted to an inverse-power relation[26,27]:

$$D \cong A\sigma^{C} \quad (1)$$

where $\sigma = Q_{Ext}/Q$Disp., and demonstrates reasonable agreement with the model (r^2 = 0.701).

The production rate (Fig. 1c) demonstrates moderate dependence on the dimensionless parameter σ, and in general, tends to increase as σ increases. Our goal was to target general mammalian cell functions so the droplet generator was designed for a nominal diameter of 10–20 μm. As a result, monodisperse double emulsions were produced with diameters ranging from 9–30 μm in a device with 20 μm tall channel features (Fig. 1d). It is possible for our design to produce double emulsions with diameters ≤ 9 μm by sacrificing some monodispersity, since below 9 μm, we could only achieve droplet formation in the jetting regime with the given orifice size. New designs to produce monodisperse populations of double emulsions down to 5 μm in diameter for in-vivo immunotherapy applications[7,28] are ongoing. The double emulsions themselves are also very robust, and can survive at least 8 months (Fig. 1e) when stored at room temperature in 1.5 mL gas-sealed vials. An increase in average diameter was noted during this period, likely due to interfacial effects from lipid degradation, though monodispersity remained consistent (Supplementary Fig. 1).

Spreading coefficient: Double emulsion storage and formation of SCMs or GUVs

Through manipulation of the interfacial tensions between the fluid phases, the equilibrium morphology of the double emulsion can be controlled (Fig. 2). The free energy of each interface can be summarized by a parameter known as the spreading coefficient (Equation

Author Manuscript Author Manuscript Author Manuscript Author Manuscript

2), which describes the tendency of a fluid phase to spontaneously spread on a solid surface (or fluid interface)[29]. Each fluid phase in the double emulsion has its own spreading coefficient that is calculated from Equation (2), where γ_{ij} represents the interfacial tensions between fluids *i* and *j*. For a double emulsion with miscible inner and outer phases, three configurations are possible: complete engulfing (double emulsion), partial engulfing (SCM), and non-engulfing (GUV + oil drop), with the conditions for each morphology described by the spreading coefficient values given in Fig. 2.

$$S_i = \gamma_{jk} - \gamma_{ik} - \gamma_{ij}, \{i, j, k\} = \{O, I, M\} \quad (2)$$

Previous analysis of the influence of the spreading coefficient on droplet morphology typically utilizes double emulsions with three immiscible fluid phases (from here on referred to as three-phase double emulsions). In a double emulsion system, an interface can only form between miscible aqueous phases if amphiphilic molecules (lipids, polymers, etc.) are present at the inner and outer oil-water interfaces that can assemble into a membrane.

Thus, for the system described herein, the value of γ_{IO} represents the tension in the resulting lipid bilayer[30]. According to Petelska *et al.*[31], the value of γ_{IO} for lipid bilayers can lie anywhere from 0.2–7 mN m^{-1}, contingent on the specific membrane composition, pH, and temperature. Given that the bilayer of the described system is composed of a 1:1 PC-lipid:cholesterol mixture, and potential residual oleic acid, an intermediate value of 3.5 mN m^{-1} was chosen for γ_{IO} in the following analysis, given that both cholesterol and fatty acids act to increase the interfacial tension relative to pure lipid bilayers. However, Petelska *et al.* only investigated the effect of cholesterol and fatty acids separately, so their effect on interfacial tension together in the same lipid bilayer was not explored. Furthermore, with measuring γ_{IO} directly, any calculation of the spreading coefficients is only useful for investigating trends between various conditions and the capability of the model to predict those trends. Interfacial tension values of the immiscible fluid phases were measured using the pendant drop method.

Complete engulfing: Double emulsion

To ensure double emulsion stability, the spreading coefficient of the outer and inner phases (S_O and S_I) must be negative, while the spreading coefficient for the middle (oil) phase (S_M) must be positive[32]. Given our assumption of the membrane tension that the formed bilayer is approximately 3.5 mN/m, possible spreading coefficient values are reported in Table 1. The values fall in line with the promotion of complete engulfing as the most energetically favorable morphology, in agreement with the results presented in Fig. 1e.

Partial engulfing: SCMs

Utilizing a method designed to extract the oil phase will facilitate the formation of a temporary SCM regardless of the spreading coefficient values. Hayward *et al.*[33] reported on the formation of SCMs during transformation of their double emulsions into polymersomes via solvent extraction. It was suggested that the driving force for the transition into SCMs was a depletion effect, whereby excess copolymer in the middle phase drove away smaller

Author Manuscript Author Manuscript Author Manuscript Author Manuscript

solvent molecules, attracting the inner and outer water-oil interfaces to form a membrane. Given that such a membrane does not form in three-phase double emulsions, depletion effects must play a significant role in the formation of the bilayer of SCMs and GUVs from double emulsion templates. As the magnitude of the depletion effect is directly related to the concentration of colloidal particles in solution (i.e., lipid molecules) a relatively high concentration of DOPC (10 mg mL^{-1}) along with cholesterol for stability (Fig. 3a,b) could facilitate conversion into SCMs (Fig. 3c) upon transfer to PBS.

The influence of increasing the interfacial tension at the external water-oil interface on SCM formation was also investigated by immersing double emulsions in isotonic solutions of sucrose, NaCl, $NaC_2H_3O_2$, and 1× PBS (Fig. 3d). Within 10 minutes, all the double emulsions in the solution of sodium acetate transitioned into SCMs, compared to less than 10% in the NaCl and NaI solutions. In PBS, approximately 50% of the double emulsions transitioned into SCMs. Upon measuring the interfacial tension between the oil phase and each aqueous solution individually, it can be seen that sodium acetate and PBS have the largest interfacial tension values (4.2 and 4.4 mN/m, respectively), while NaCl and sucrose are lower (2.2 and 1.7 mN/m, respectively) suggesting the increase in interfacial tension at the outer water-oil interface plays a role in SCM formation. A possible explanation is that the increased interfacial tension forces the oil phase to adopt a more thermodynamically favorable morphology by reducing the surface area of the most energetically costly interface, whereby it accumulates at one region of the double emulsion to form an SCM Supplementary Fig. 2a. The high local concentration of lipids in the thinning portion of the middle layer further promotes bilayer formation via a depletion effect[33]. SCMs formed in different aqueous solutions can be seen in Supplementary Fig. 2b, and possible spreading coefficients are summarized in Table 2.

For the SCM morphology to be energetically favored, all three spreading coefficients must be negative according to the model (Fig. 2). From Table 2, it can be seen that increasing the interfacial tension at the outer water-oil interface decreases the value of S_M relative to the storage solution (Table 1), in agreement with the model's prediction. The depletion effect likely also has an influence as the oil shell of the double emulsion thins, and could be enough to cause SCM formation in structures that are close to the transformation point, causing deviation from the model. Reducing the surfactant concentration in the internal phase further reduced S_M and S_I, suggesting that the likelihood of conversion into an SCM was further increased by increasing the interfacial tension at the internal water-oil interface as well (Table 3).

The SCMs are also fairly stable, surviving long enough to allow experiments to be conducted even a day later. More than 90% of the SCMs survived after 24 hours in PBS, and 70% of the population was still present after 48 hours (Fig. 3e), in agreement with survival rates reported by Villar *et al.*[30] The fluorescent molecule FITC-Dextran was also included in the internal phase of the SCMs to demonstrate they can hold encapsulated material (Supplementary Fig. 3).

Author Manuscript Author Manuscript Author Manuscript Author Manuscript

Non-engulfing: GUVs

According to the spreading coefficient model, oil cap separation from the SCM can be achieved when $S_O > 0$ and both S_I and $S_M < 0$. Essentially, this means that γ_{IM} becomes considerably larger than either γ_{IO} or γ_{MO}, [$\gamma_{IM} > (\gamma_{IO} + \gamma_{MO})$, Equation 3], so that the interface formed between the oil phase and the internal water phase becomes energetically unfavorable. To achieve this criterion, the amount of encapsulated surfactant was reduced to 1%, and sucrose was replaced with 1× PBS in the internal phase. Furthermore, since a depletion effect drives bilayer formation, DPPC (1,2-dipalmitoyl-sn-glycero-3-phosphocholine, Avanti Polar Lipids) was included in the middle phase at a 50% molar ratio to increase the favorability of GUV formation. Since DOPC and oleic have very similar structures, with each having 18 carbons in their tail(s) and a single double bond, it was theorized that adding a lipid with a comparatively dissimilar structure may enhance depletion and bilayer formation. DPPC has a fully saturated 16-carbon chain in each tail, and has a higher phase transition temperature than DOPC. Furthermore, solubility of DPPC in oleic acid was noticed to be lower compared to DOPC, suggesting DPPC may be more likely to dissociate from the oleic acid solvent and organize among itself during dewetting to form a bilayer. Since DPPC would be in the gel-crystalline phase when incorporated into lipid bilayers at room temperature, it could also act to enhance the robustness of SCMs and GUVs.

The first step to promote non-engulfing was to increase the value of γ_{IM}, which was accomplished by introducing an osmotic pressure difference to cause the double emulsions to shrink and increase the internal electrolyte concentration, presumably increasing γ_{IM} as a result. After approximately 15 minutes of placement in either 2× PBS or > 0.6 Osm KCl, the double emulsions shrunk considerably, and began to transition into SMCs, and then GUVs (Supplementary Fig. 4). The estimated spreading coefficient values of the double emulsions before and after shrinkage are listed in Supplementary Table 1. As the double emulsions shrink, S_O becomes more positive, while both S_M and S_I become more negative. Assuming the trend would continue, the conditions for the non-engulfing morphology in Fig. 2 would be met. It's also likely the enhancement to the depletion effect could play a role in promoting the non-engulfing morphology, as repeating the experiment without DPPC showed no cap removal in 0.6 Osm KCl, even after 15 minutes (Supplementary Fig. 5).

Another route to promote non-engulfing is to decrease γ_{MO}. To achieve this, double emulsions that contained DPPC were added to a solution of sucrose with a high concentration of surfactant (~10% F68) to force γ_{MO} to approach 0 mN m^{-1}, reducing Equation 3 to $\gamma_{IM} > \gamma_{IO}$ (Equation 4). Furthermore, subjecting the double emulsions to a hypertonic solution to cause shrinkage could further help to dynamically increase the concentration of electrolyte in the aqueous core to increase γ_{IM}. As can be seen in Supplementary Fig. 6a, the oil phase of the double emulsions immediately began to escape as small drops. It's probable that this observation is due to the formation of many small oil caps that are each then separating from the SCM individually. Since the interfacial tension at the outer water-oil interface was exceedingly small, any small perturbations, shear, or drag could cause oil breakup due to an increase in the localized capillary number. Upon introducing shear forces to the system by washing with excess solution, significant

Author Manuscript Author Manuscript Author Manuscript Author Manuscript

membrane thinning and possible GUVs could be seen Supplementary Fig. 6b. The small dark regions on the corner of some drops could be excess lipid or residual oil.

Upon introduction into a solution of 2× PBS with 50% glycerol, the double emulsions (1:1 molar ratio DOPC:DPPC, 10 mg/mL total lipid, 2.5 mg/mL cholesterol) successfully underwent a transition from SCMs to GUVs via removal of the oil cap (Fig. 4). Further work is underway to elucidate the specific affect glycerol had to cause this phenomenon. Given the partial miscibility of glycerol in oleic acid, possible explanations include migration to the internal aqueous core to also act on the internal oil-water interface or an influence on the solubility of the dissolved lipids to improve depletion.

NL-2 functionalized SCMs elicit increases in pancreatic B-cell insulin secretion and cellular growth

To investigate the ability of CLVs to be utilized as artificial cells, SCMs were functionalized with a protein complex that consisted of the extracellular domain of NL-2, a transmembrane protein expressed in β cells (Fig. 5a). The NL-2 functionalized SCMs were added to the culture medium of pancreatic β cells to determine effects on insulin secretion and cell growth. Exogenously administered monomeric soluble NL-2 has been shown to decrease insulin secretion. Clustered NL-2, however, is known to increase stimulated insulin secretion, but may need to be anchored to a fluid, spherical surface to be effective[9,34,35].

NL-2 functionalized SCMs were able to mimic the transcellular effects on β cells of co-cultured HEK293 cells expressing NL-2 on their plasma membrane[35]. Glucose-stimulated insulin secretion in 832/13 cells was significantly increased ($p < 0.01$, $n = 6$) after 24-hour incubation (Fig. 5b). Likewise, incubation with NL-2 functionalized SCMs resulted in significant increases ($p < 0.001$, $n = 11$) in cell growth (Fig. 5c). The increase in cellular protein level likely indicates a cellular proliferation effect, as previously shown with NL-2 co-culture and nanoparticle studies[34,35].

CONCLUSION

We have presented a microfluidic technique capable of producing storable, cell-sized CLVs that can be functionalized for biological activity either via surface modification and/or the inclusion of bioactive molecules in the aqueous interior or lipophilic shell. The CLVs possess unilamellar lipid bilayer membranes and can be produced with a wide range of uniform sizes through control of the flow-rates/applied pressures of the various component phases. After production, fragile molecules and biological components can be added to the surface for functionalization, or encapsulated into the SCMs using standard nano-vesicle fusion techniques[36,37]. Double emulsions can also be pre-functionalized or made to contain a stable drug compound before storage and then converted into CLVs at a later date when ready for use, allowing functional CLVs to be made in bulk and distributed to a wide variety of consumers for use as a cellular therapies, biosensors, and artificial cells.

Artificial cells in particular hold great promise in that they can serve as biomimetic platforms for molecular synthesis, cell-cell signaling and cell-based therapies. For example, CLVs with a fluid surface that can be functionalized to interact and influence the behavior of

Author Manuscript Author Manuscript Author Manuscript Author Manuscript

cells present an interesting class of biomimetic structures that have immense therapeutic potential. The coordinated arrangement of ligand-receptor pairs into ordered spatial patterns on the cell surface has recently been recognized as a recurring theme that occurs in many juxtacrine-signaling pathways, and presents a paradigm shift from the concept of static cellular surface interactions[5,6]. The importance of fluid micro-domains in cell-to-cell communication is widely recognized in the immune synapse formed when antigen-presenting cells interact with T-cells, and is a prominent design criterion in the creation of artificial antigen presenting cells (aAPCs) for immunotherapy[8].

In addition to the immune synapse, the neurexin-neuroligin signaling pathway is another system that has been discovered to rely on ligand-receptor clustering and mobility. Neurexins are a family of neuronal surface receptors that aid in neural synapse formation. In particular, β-neurexins are a class of receptors that bind to neuroligin-1, a postsynaptic cell surface protein[38]. Clustering of neuroligin-1 (or neuroligin-2) on the post-synaptic membrane induces clustering of presynaptic axonal neurexins, the result of which is synaptic maturation and neurotransmitter secretion. Baksh *et al.*[9] verified the significance of this clustering effect by culturing neurons with both silica beads coated with neuroligin-1-containing lipid bilayers and naked polystyrene beads with covalently bonded neuroligin-1. Only the beads with neuroligin-1-containing lipid bilayers were biologically active, while the beads lacking a lipid membrane did not provide any activation.

Interestingly, pancreatic β cells also utilize a neuroligin transcellular signaling system, expressing much of the same cellular components and proteins that are important for neurotransmitter secretion and repurposing them for the secretion of insulin[35,39]. Specifically, pancreatic β cells express NL-2 (expressed in inhibitory synapses in the nervous system), which is known to bind transcellularly with neurexin on neighboring cells[40]. Neuroligin induces neighboring cells to proliferate at a higher rate and secrete higher levels of insulin[34,35], with both effects having therapeutic potential for Type 2 diabetics. Neuroligin's insulin secretion effect may be independent of interactions with neurexins[35].

NL-2 is likely exerting its insulin secretory effect in a manner similar to its effects on neurotransmitter release, namely that clustering of NL-2 on the β cell surface increases the insulin secretory capacity of neighboring β cells during cell-to-cell contact[35]. Furthermore, as is the case with the membrane components that comprise the immune synapse, monomeric NL-2 in solution is unable to exert its clustered effect and can hinder insulin secretion[35]. This presents an ideal opportunity for GUV or SCM based artificial cells in applications that require a biomimetic cell surface.

Supplementary Material

Refer to Web version on PubMed Central for supplementary material.

Acknowledgments

This work was funded in part by the National Institute of Health, Grant No's. R01-EB012058 and R01-DK080971, and the UC Irvine Department of Medicine Chair's Award. The authors would also like to thank Dr. Ken Shea for access to the SPEX Fluorolog 1680 0.22 m Dual Spectrometer.

Author Manuscript Author Manuscript Author Manuscript Author Manuscript

References

1. Curtsinger J, Deeths MJ, Pease P, Mescher MF. Artificial cell surface constructs for studying receptor-ligand contributions to lymphocyte activation. J Immunol Methods. 1997; 209:47–57. [PubMed: 9448033]
2. Shen CL, et al. Latex bead-based artificial antigen-presenting cells induce tumor-specific CTL responses in the native T-cell repertoires and inhibit tumor growth. Immunol Lett. 2013; 150:1–11. [PubMed: 23328744]
3. Chiu YL, Schneck JP, Oelke M. HLA-Ig based artificial antigen presenting cells for efficient ex vivo expansion of human CTL. J Vis Exp. 2011; (50):2801. pii. [PubMed: 21505415]
4. Steenblock ER, Fahmy TM. A comprehensive platform for ex vivo T-cell expansion based on biodegradable polymeric artificial antigen-presenting cells. Mol Ther. 2008; 16:765–772. [PubMed: 18334990]
5. Groves JT. Molecular organization and signal transduction at intermembrane junctions. Angew Chem Int Edit. 2005; 44:3524–3538.
6. Davis MM, et al. Dynamics of cell surface molecules during T cell recognition. Annu Rev Biochem. 2003; 72:717–742. [PubMed: 14527326]
7. Giannoni F, et al. Clustering of T cell Ligands on artificial APC membranes influences T cell activation and protein kinase C theta translocation to the T cell plasma membrane. J Immunol. 2005; 174:3204–3211. [PubMed: 15749850]
8. Eggermont LJ, Paulis LE, Tel J, Figdor CG. Towards efficient cancer immunotherapy: Advances in developing artificial antigen-presenting cells. Trends Biotechnol. 2014; 32:456–465. [PubMed: 24998519]
9. Baksh MM, et al. Neuronal activation by GPI-linked neuroligin-1 displayed in synthetic lipid bilayer membranes. Langmuir. 2005; 21:10693–10698. [PubMed: 16262338]
10. Bouvrais H, Pott T, Bagatolli LA, Ipsen JH, Méléard P. Impact of membrane-anchored fluorescent probes on the mechanical properties of lipid bilayers. Biochim Biophys Acta. 2010; 1798:1333–1337. [PubMed: 20398624]
11. Ohlsson G, et al. Solute transport on the sub 100 ms scale across the lipid bilayer membrane of individual proteoliposomes. Lab Chip. 2012; 12:4635–4643. [PubMed: 22895529]
12. Yoshitani, T., Yamazaki, M. International Symposium on Micro-NanoMechatronics and Human Science (MHS 2008). Nagoya, Japan: IEEE; New Jersey: Nov 6–9, 2008. Water permeability of lipid membranes of GUVs and its dependence on actin cytoskeletons inside the GUVs; p. 130-134.2008
13. Budin I, Szostak JW. Physical effects underlying the transition from primitive to modern cell membranes. Proc Natl Acad Sci USA. 2011; 108:5249–5254. [PubMed: 21402937]
14. Richmond DL, et al. Forming giant vesicles with controlled membrane composition, asymmetry, and contents. Proc Natl Acad Sci USA. 2011; 108:9431–9436. [PubMed: 21593410]
15. De Souza Pereira T, Stano P, Luisi PL. The minimal size of liposome-based model cells brings about a remarkably enhanced entrapment and protein synthesis. Chembiochem. 2009; 10:1056–1063. [PubMed: 19263449]
16. Murtas G, Kuruma Y, Bianchini P, Diaspro A, Luisi PL. Protein synthesis in liposomes with a minimal set of enzymes. Biochem Biophys Res Commun. 2007; 363:12–17. [PubMed: 17850764]
17. Jimenez M, Martos A, Cabre EJ, Raso A, Rivas G. Giant vesicles: A powerful tool to reconstruct bacterial division assemblies in cell-like compartments. Environ Microbiol. 2013; 15:3158–3168. [PubMed: 23944240]
18. Fenz SF, Sengupta K. Giant vesicles as cell models. Integr Biol (Camb). 2012; 4:982–995. [PubMed: 22829218]
19. Xia YN, Whitesides GM. Soft lithography. Angew Chem Int Edit. 1998; 37:551–575.
20. Kozlov M, Quarmyne M, Chen W, McCarthy TJ. Adsorption of poly(vinyl alcohol) onto hydrophobic substrates. A general approach for hydrophilizing and chemically activating surfaces. Macromolecules. 2003; 36:6054–6059.

Author Manuscript Author Manuscript Author Manuscript Author Manuscript

21. Teh SY, Khnouf R, Fan H, Lee AP. Stable, biocompatible lipid vesicle generation by solvent extraction-based droplet microfluidics. Biomicrofluidics. 2011; 5:044113.
22. Martz TD, Bardin D, Sheeran PS, Lee AP, Dayton PA. Microfluidic generation of acoustically active nanodroplets. Small. 2012; 8:1876–1879. [PubMed: 22467628]
23. Comoletti D, et al. Gene selection, alternative splicing, and post-translational processing regulate neuroligin selectivity for beta-neurexins. Biochemistry. 2006; 45:12816–12827. [PubMed: 17042500]
24. Zhang C, et al. Extracellular CADM1 interactions influence insulin secretion by rat and human islet beta-cells and promote clustering of syntaxin-1. Am J Physiol Endocrinol Metab. 2016; 310:E874–E885. [PubMed: 27072493]
25. Hettiarachchi K, Lee AP, Zhang S, Feingold S, Dayton PA. Controllable micro-fluidic synthesis of multiphase drug-carrying lipospheres for site-targeted therapy. Biotechnol Progr. 2009; 25:938–945.
26. Ward T, Faivre M, Abkarian M, Stone HA. Microfluidic flow focusing: Drop size and scaling in pressure versus flow-rate-driven pumping. Electrophoresis. 2005; 26:3716–3724. [PubMed: 16196106]
27. Bardin D, et al. High-speed, clinical-scale microfluidic generation of stable phase-change droplets for gas embolotherapy. Lab Chip. 2011; 11:3990–3998. [PubMed: 22011845]
28. Ugel S, et al. In vivo administration of artificial antigen-presenting cells activates low-avidity T cells for treatment of cancer. Cancer Res. 2009; 69:9376–9384. [PubMed: 19934317]
29. Guzowski J, Korczyk PM, Jakiela S, Garstecki P. The structure and stability of multiple micro-droplets. Soft Matter. 2012; 8:7269–7278.
30. Villar G, Heron AJ, Bayley H. Formation of droplet networks that function in aqueous environments. Nat Nanotechnol. 2011; 6:803–808. [PubMed: 22056724]
31. Petelska AD. Interfacial tension of bilayer lipid membranes. Central Eur J Chem. 2012; 10:16–26.
32. Torza S, Mason SG. 3-Phase interactions in shear and electrical fields. J Colloid Interface Sci. 1970; 33:67–83.
33. Hayward RC, Utada AS, Dan N, Weitz DA. Dewetting instability during the formation of polymersomes from block-copolymer-stabilized double emulsions. Langmuir. 2006; 22:4457–4461. [PubMed: 16649747]
34. Munder A, et al. Mimicking neuroligin-2 functions in beta-cells by functionalized nanoparticles as a novel approach for antidiabetic therapy. ACS Appl Mater Interfaces. 2017; 9:1189–1206. [PubMed: 28045486]
35. Suckow AT, et al. Transcellular neuroligin-2 interactions enhance insulin secretion and are integral to pancreatic beta cell function. J Biol Chem. 2012; 287:19816–19826. [PubMed: 22528485]
36. Tsumoto, K., et al. International Symposium on Micro-NanoMechatronics and Human Science (MHS 2009). Nagoya, Japan: IEEE; New Jersey: Nov 9–11, 2009. G protein coupled receptors (GPCRs) reconstituted on recombinant proteoliposomes using baculovirus-liposome membrane fusion; p. 202-207.2009
37. Csiszá r A, et al. Novel fusogenic liposomes for fluorescent cell labeling and membrane modification. Bioconjug Chem. 2010; 21:537–543. [PubMed: 20184308]
38. Dean C, et al. Neurexin mediates the assembly of presynaptic terminals. Nat Neurosci. 2003; 6:708–716. [PubMed: 12796785]
39. Easom RA. Beta-granule transport and exocytosis. Semin Cell Dev Biol. 2000; 11:253–266. [PubMed: 10966859]
40. Mosedale M, Egodage S, Calma RC, Chi NW, Chessler SD. Neurexin-1 alpha contributes to insulin-containing secretory granule docking. J Biol Chem. 2012; 287:6350–6361. [PubMed: 22235116]

Author Manuscript Author Manuscript Author Manuscript Author Manuscript

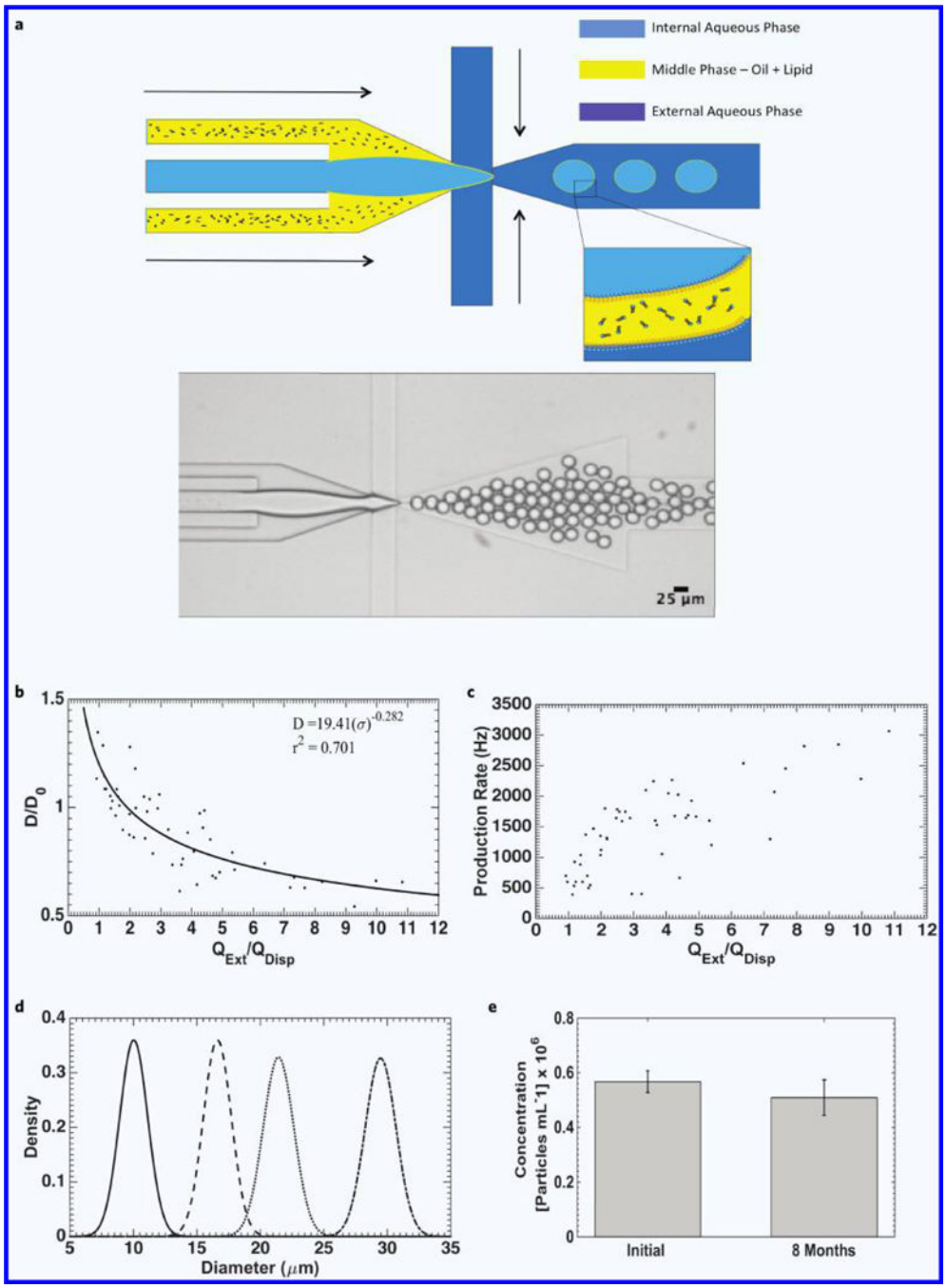

Figure 1.

Double emulsion production and characterization. (**a**) Schematic of double emulsion production (top) and brightfield image of double emulsion generation zone and double emulsion production (bottom). (**b**) Droplet diameter normalized to orifice length (D/D_0) as a function of external phase flow (Q_{Ext}) normalized to the sum of the dispersed phase flow rates (Q_{Disp}). (**c**) Droplet generation rate as a function of normalized flow rate. (**d**) Population distribution of double emulsions at various diameters. From left-to-right: (Mean

Author Manuscript Author Manuscript Author Manuscript Author Manuscript

± STD) 10.1 ± 1.1 μm, 16.6 ± 1.1 μm, 21.4 ± 1.2 μm, 28.5 ± 1.5 μm. (**e**) Double emulsion population after eight months of storage at room temperature ($p = 0.0926$, $n = 8$).

Author Manuscript Author Manuscript Author Manuscript Author Manuscript

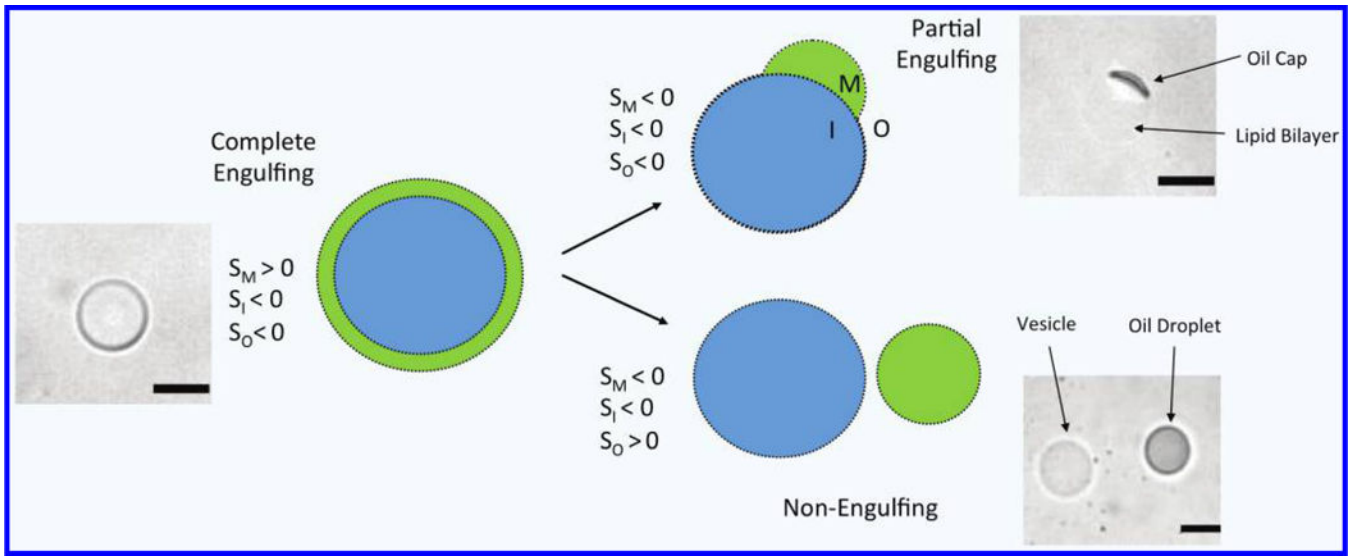

Figure 2.

Illustration and phase contrast images of possible double emulsion equilibrium morphologies based on the values of the spreading coefficient for each fluid phase. Scale bars are 20 μm.

Author Manuscript Author Manuscript Author Manuscript Author Manuscript

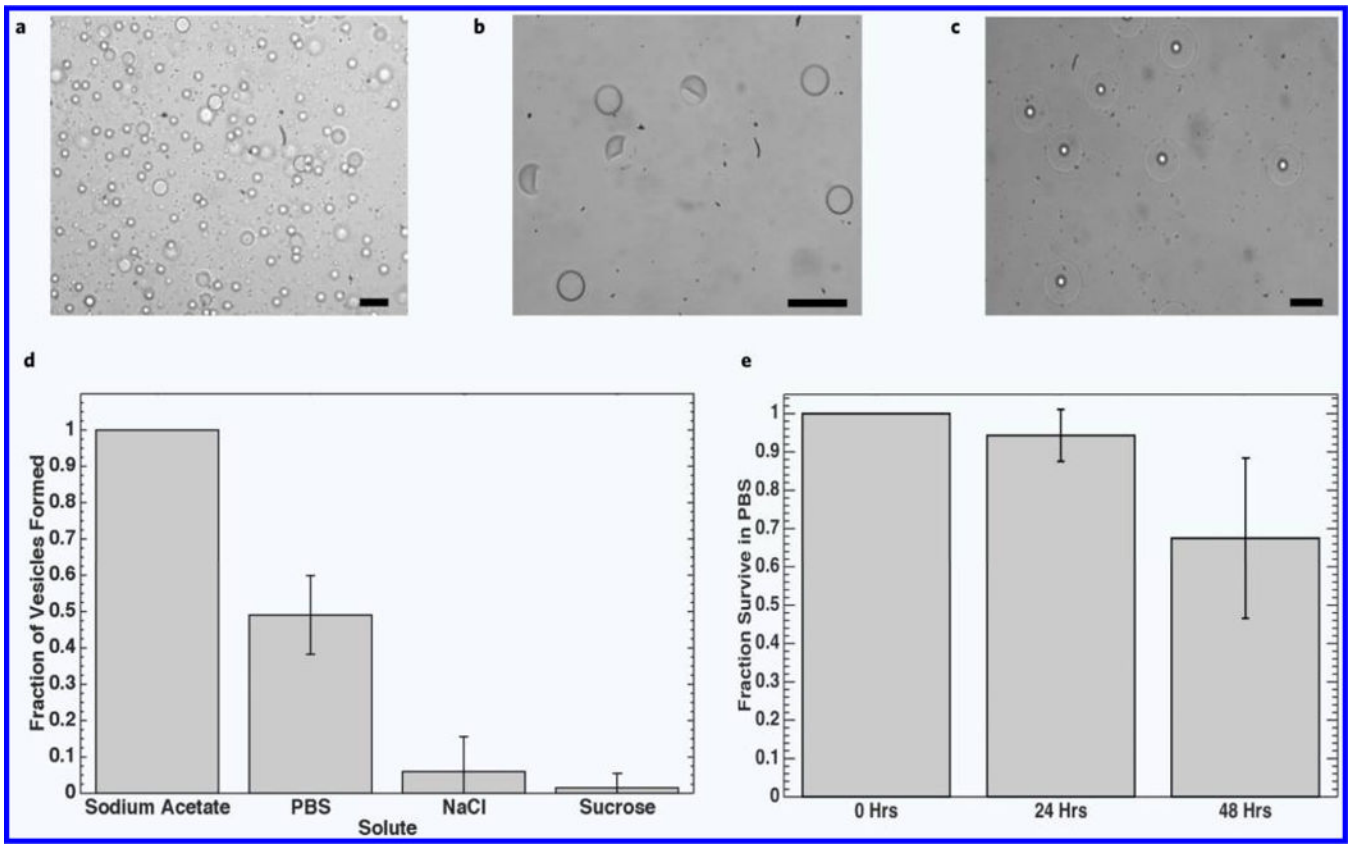

Figure 3.

Phase contrast images demonstrating effect of lipid and cholesterol concentration on SCM formation in 1× PBS. (**a**) 5 mg mL^{-1} DOPC in middle phase. (**b**) 5 mg mL^{-1} DOPC + 2.5 mg mL^{-1} cholesterol in middle phase. (**c**) 10 mg mL^{-1} DOPC + 5 mg mL^{-1} cholesterol in middle phase. Dewetting characteristics and vesicle survival. (**d**) Fraction of vesicles seen after 10 minutes in various electrolytic solutions ($n = 4$). No dewetting was observed when vesicle solution was diluted with deionized water. (**e**) Survival characteristic of vesicles in PBS after dewetting ($n = 9$). Scale bars are 50 μm.

Author Manuscript Author Manuscript Author Manuscript Author Manuscript

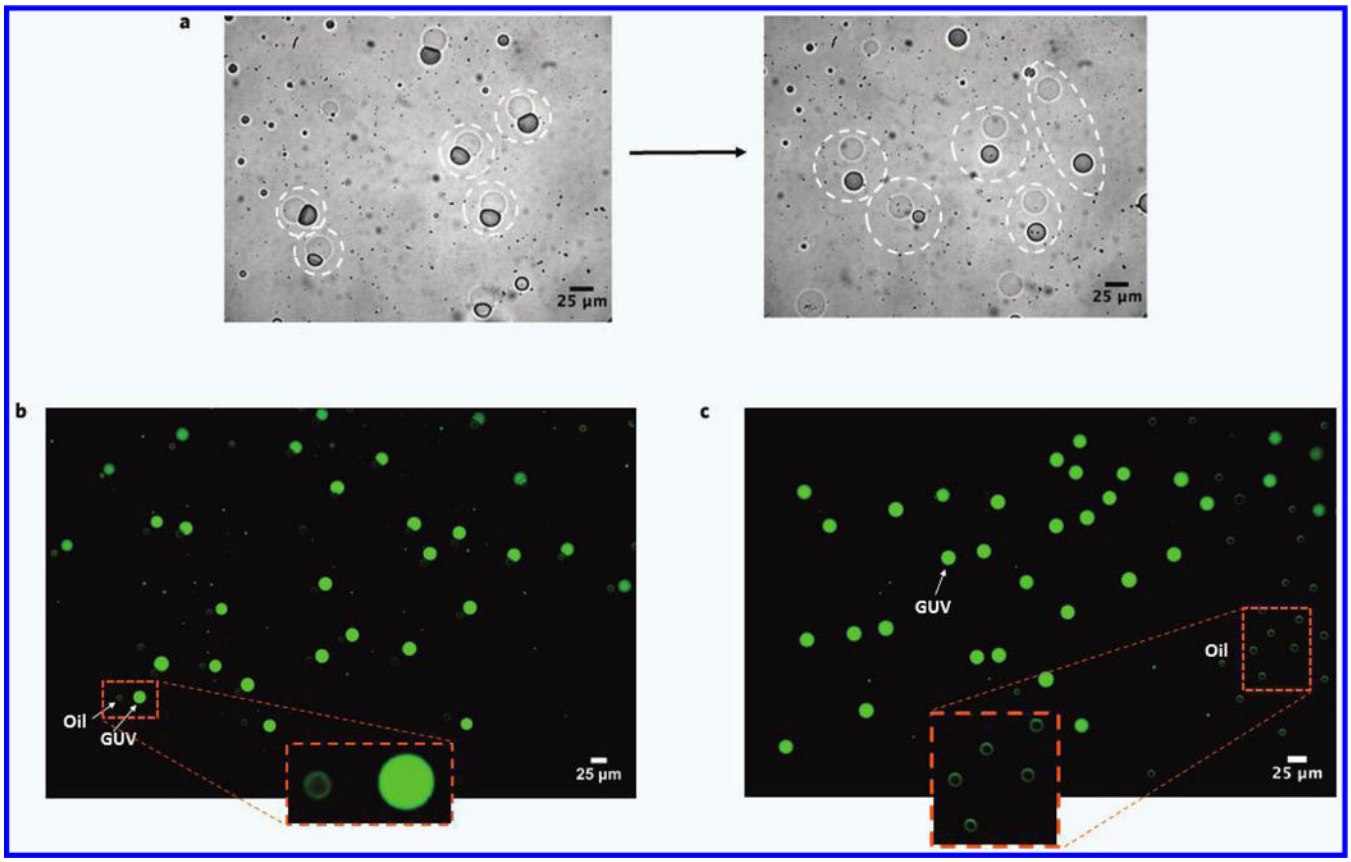

Figure 4.

Formation of GUVs. (**a**) Phase contrast images SCMs shedding their oil caps to become GUVs in solution with high surfactant concentration. Before and after GUV-Oil drop pairs are indicated by the dashed circles. (**b**) Fluorescent image showing population of GUVs just after separation from oil cap. Internal phase contained 100 μM FITC-Dextran. Small, faint green drops are the oil caps, which are visible due to the slight introduction of brightfield light through the FITC filter. Background is subtracted. (**c**) Fluorescent image taken in the same manner as in (**b**), showing a population of GUVs (left) that have drifted away from their oil caps (right).

Author Manuscript Author Manuscript Author Manuscript Author Manuscript

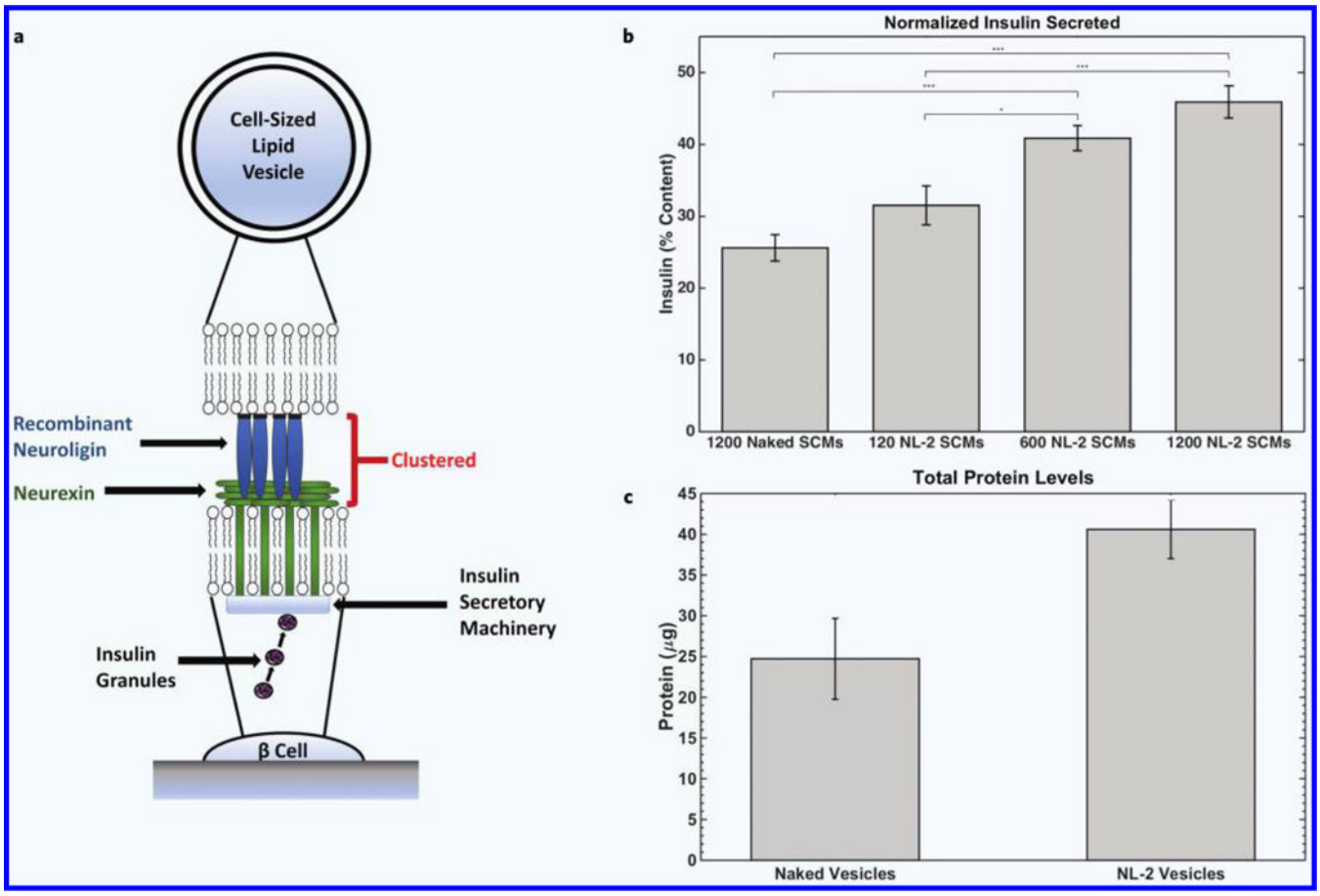

Figure 5.

(**a**) Illustration of proposed β cell interaction with NL-2 functionalized SCM. (**b**) Dose-dependent insulin secretion (normalized to cellular insulin content) from pancreatic β cells after 24-hour incubation with NL-2 functionalized SCMs. Insulin secretion increased with greater number of functionalized SCMs, demonstrating the biomimetic potential of NL-2 functionalized SCMs for antidiabetic therapy ($p < 0.01$, $n = 6$). (**c**) Protein levels from pancreatic β cells after 24-hour incubation with naked and NL-2 functionalized SCMs. NL-functionalized SCMs significantly increased protein levels ($p < 0.001$, $n = 11$), further demonstrating the biological activity of NL-2 functionalized SCMs.

Author Manuscript

Author Manuscript

Author Manuscript

Author Manuscript

Table 1

Spreading coefficients for double emulsions in external solution where double emulsion morphology is maintained.

Internal Phase: 0.25 Osm Sucrose + 5% F68 **Middle Phase: 10 mg mL^{-1} DOPC + 5 mg mL^{-1} Cholesterol in Oleic Acid**	S_O	S_M	S_I
Storage Solution	−5.18	1.74	−1.82
0.25 Osm Sucrose	−6.58	0.34	−0.42
0.25 Osm Sucrose + 5% F68	−3.50	3.42	−3.50

Author Manuscript

Author Manuscript

Author Manuscript

Author Manuscript

Table 2

Spreading coefficients for double emulsions in external solution where SCM morphology is promoted.

Internal Phase: 0.25 Osm Sucrose + 5% F68 **Middle Phase: 10 mg mL^{-1} DOPC + 5 mg mL^{-1} Cholesterol in Oleic Acid**	S_O	S_M	S_I
1× PBS	−7.86	−2.15	0.86
0.25 Osm Sodium Acetate	−7.69	−0.77	0.69
0.25 Osm NaCl	−5.65	1.28	−1.35

Author Manuscript

Author Manuscript

Author Manuscript

Author Manuscript

Table 3

Spreading coefficients for double emulsions in external solution where SCM morphology is promoted. Surfactant concentration in the internal phase is reduced.

Internal Phase: 1× PBS + 1% F68 **Middle Phase: 10 mg mL^{-1} DOPC + 5 mg mL^{-1} Cholesterol in Oleic Acid**	S_O	S_M	S_I
1× PBS	−5.18	−3.62	−1.82
0.25 Osm Sodium Acetate	−5.02	−3.45	−1.98
0.25 Osm NaCl	−2.97	−1.40	−4.03